JOURNAL OF AGRICULTURAL AND FOOD CHEMISTRY

Article

pubs.acs.org/JAFC

Structural and Physicochemical Property Relationships of Cruciferin Homohexamers

Thushan S. Withana-Gamage,[†,‡] Dwayne D. Hegedus,[†,‡] Xiao Qiu,[‡] Tara McIntosh,[†] and Janitha P.D. Wanasundara*[,†,‡]

[†]Agriculture and Agri-Food Canada, Saskatoon, Saskatchewan, S7N 0X2 Canada

[‡]Department of Food and Bioproduct Sciences, University of Saskatchewan, Saskatoon, Saskatchewan, S7N 5A9 Canada

Supporting Information

ABSTRACT: Heteromeric cruciferin from wild type (WT) *Arabidopsis thaliana* and homomeric cruciferin CRUA, CRUB, and CRUC composed of identical subunits obtained from double-knockout mutant lines were investigated for their structural and physicochemical properties. A three-step chromatographic procedure allowed isolation of intact cruciferin hexamers with high purity (>95%). FT-IR and CD analysis of protein secondary structure composition revealed that all cruciferins were folded into higher order structures consisting of 44−50% β-sheets and 7−9% α-helices. The structural and physicochemical properties of homohexameric CRUC deviated from that of CRUA and CRUB and exhibited a compact, thermostable, and less hydrophobic structure, confirming the predictions made using 3D homology structure models.

KEYWORDS: *cruciferin, Arabidopsis thaliana, 3D homology structure, homohexamer, physicochemical properties*

INTRODUCTION

Cruciferin is the predominant seed storage protein of crucifer oilseeds, such as canola/rapeseed and mustard. As such, it is a very important contributor to the nutritional and functional properties of the crucifer seed protein fraction. Cruciferin is an 11−12S globulin and has a hexameric quaternary structure composed of six subunits (protomers). Each protomer consists of two polypeptides, an α- (acidic) and β- (basic) chain.[1] The wild type (WT) cruciferin is a heterogeneous mixture of subunits contributed by families of homologous genes. Therefore, cruciferin isolated from a natural crucifier is an undefined mixture of these subunits. In *Brassica napus* L., at least five different cruciferin subunits have been reported, denoted as CRUA (CRU2/3), CRU1, CRU2, CRU3, and CRU4,[2,3] although transcriptional studies indicate that the genome contains at least 12 cruciferin genes (Hegedus, unpublished). Understanding the structure and structure-related functions of cruciferin protomers will greatly assist in improving the utility of the crucifer protein fraction; however, data obtained from WT cruciferin does not allow assessments of each protomer type as it is a mixture of several subunit variants.

Current understanding of the structural, physicochemical, and functional properties of cruciferin is limited to a procruciferin CRU2/3a trimer subunit that was expressed in *Escherichia coli*.[1,4−6] In bacteria, procruciferin is not post-translationally processed by asparaginyl endopeptidase that occurs in plants. Using the glycinin (11S protein from soy bean) protomer, Dickinson et al. [7] showed that post-translational cleavage is necessary for final assembly of the hexamer in protein storage vacuoles. Also, the spatial position of hypervariable or disordered region IV (HVR-IV) of the glycinin protomer changes upon post-translational processing,[8] indicating that different regions of the molecule are exposed in the mature hexamer compared to the pro-trimeric structure. The HVRs play a vital role in physicochemical properties of the molecule and therefore the techno-functional properties and bioavailability of amino acids.[4,6,9,10] Furthermore, properties such as electrostatic potential and hydrophobicity in interchain (IE) and intrachain (IA) faces of cruciferin and procruciferin are distinctly different,[8,10] and may affect the ability of the protein to interact with other proteins and nonprotein components.

Understanding the structure−function relationships of major crucifer storage proteins at the subunit level will help to improve protein quality for targeted applications for oilseeds including food crops such as canola and biofuel crops such as *Brassica carinata* and *Camelina sativa*. To generate this information, we developed mutant *Arabidopsis* lines in which two of the three genes encoding cruciferin subunits (AT5G44120.3, AT1G03880.1, and AT4G28520.1) were inactivated by T-DNA insertion yielding lines producing cruciferin composed of a single subunit (CRUA, CRUB, or CRUC). The objective of this study was to probe the structure of these homomeric cruciferins at the secondary and tertiary structure level and correlate this with key physicochemical properties important for techno-functionalities of these proteins.

MATERIALS AND METHODS

Plant Materials. *Arabidopsis thaliana* (ecotype Columbia) cruciferin double-knockout lines (*CRUAcruBcruC* or *CRUAbc*, *cruACRUBcruC* or *CRUaBc*, and *cruAcruBCRUC* or *CRUabC*), triple-knockout line (*cruAcruBcruC* or *CRUabc* or *CRU-*), and wild

Received: February 4, 2013
Revised: May 8, 2013
Accepted: May 21, 2013
Published: May 21, 2013

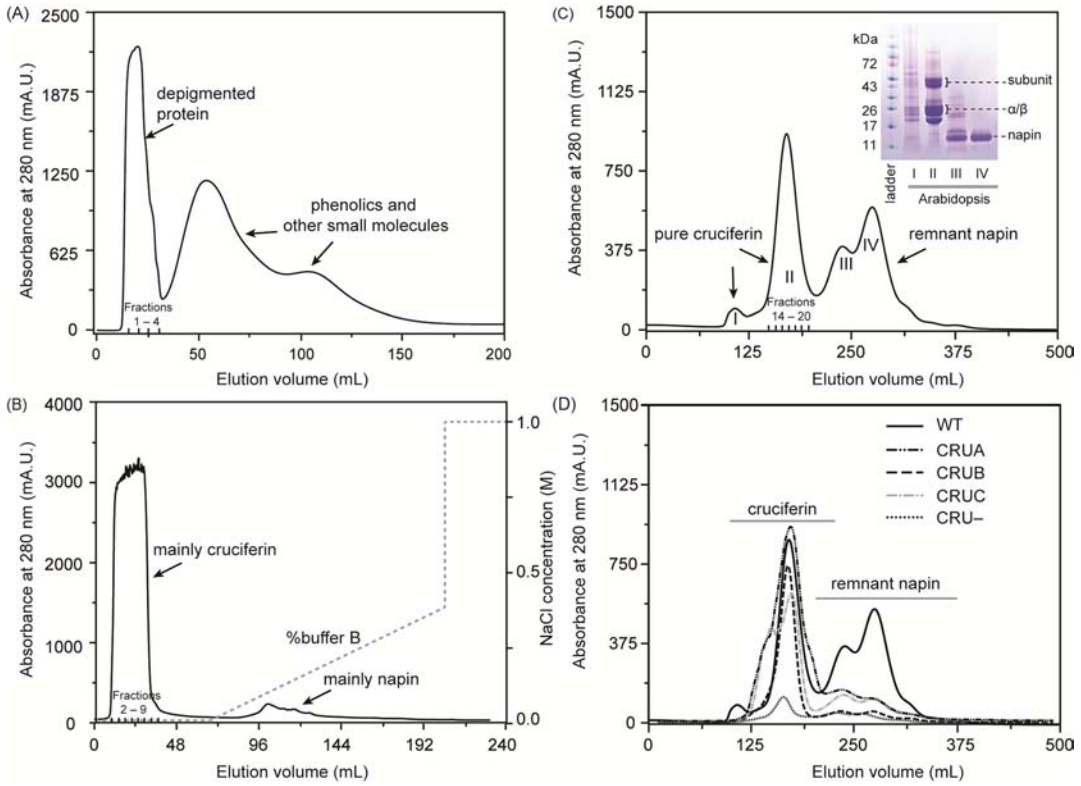

Figure 1. Chromatographic separation of *Arabidopsis* protein extracts. (A) Depigmentation by SEC on a Sephadex G-25 column. Fractions 1−4 are essentially total proteins. (B) Fractionation of the total proteins by CEC on a Resource S column. Unbound protein (mainly cruciferin) eluted in fractions 2−9, and bound fraction (mainly napin) eluted with a NaCl gradient in buffer B. (C) Purification of the CEC cruciferin fraction by SEC on a Sephacryl S-300 column. Inset: SDS-PAGE separation from left to right, MW ladder, peaks I, II, III, and IV under nonreducing conditions. The symbol α/β denotes non-cross-linked α and β polypeptide chains. (D) Overlay of chromatogram from all four cruciferins after the final SEC.

type (WT) (*CRUACRUBCRUC* or *CRUABC*) seeds were propagated under controlled greenhouse conditions (16 h ~800 Wm^2 light at 21 °C and 8 h dark at 16 °C) as described by Withana-Gamage et al.[11]

Isolation and Purification of Cruciferin. Isolation and purification of cruciferin from *Arabidopsis* seeds were as described by Bérot et al.[12] with the modifications adopted by Wanasundara et al.[13] Preparation of defatted seed meal was carried out using Swedish tube method (AOCS AM 2-93)[14] with hexane as the solvent (3 g of seeds and 25 mL of hexane). Oil-free meal was recovered by filtering the hexane meal slurry through Whatman #1 filter paper and subsequently dried under a fume hood to remove hexane. Protein extracts from defatted meals (1:10, w/v meal to buffer, ambient temperature, 1 h with mixing) were prepared with 50 mM Tris-HCl (pH 8.5), 750 mM NaCl, 5 mM EDTA, and 0.3% (w/v) $NaHSO_3$, containing EDTA-free protease inhibitor cocktail (0.02 tablet mL^{-1}) (Roche Diagnostics GmbH, Germany). The supernatant was recovered by centrifugation (15 000 × *g* for 10 min) and the pellet re-extracted under same conditions. The supernatants were combined and stored at −20 °C.

Seed extract was first passed through a Sephadex G-25 HiPrep 26/10 desalting column (2.6 cm × 10 cm, 53 mL, protein load of 70 mg protein/mL gel, equilibration and elution buffer of 50 mM Tris-HCl containing 1 M NaCl at pH 8.5, 0.2−0.5 mL min^{-1} isocratic flow rate) to remove coextracted pigments and small molecular weight compounds. The depigmented protein fraction (1−4, Figure 1A) was dialyzed (2 kDa MWCO) against deionized water for 48 h at 4 °C (3−4 water changes) and then lyophilized. Reconstituted protein fraction was then fractionated on a cation exchange column (CEC, Resource S methyl sulfonate attached to polystyrene/divinyl benzene, 1.6 cm × 9.2 cm, 18.5 mL) equilibrated with elution buffer A [50 mM Tris-HCl, 5 mM EDTA, 0.3% (w/v) $NaHSO_3$, pH 8.5] at a flow rate of 2.5 mL min^{-1} and protein load of 25 mg protein/mL gel. The unbound fractions 2−9 (Figure 1B) were combined, and dialyzed in the same manner as above and then freeze-dried. Adsorbed proteins were eluted using buffer B [50 mM Tris-HCl, 5 mM EDTA, 0.3% (w/v) $NaHSO_3$, 1 M NaCl, pH 8.5] at a linear gradient of 5% to 35% NaCl. The unbound protein was further purified on a Sephacryl S-300 HiPrep 26/10 high-resolution column (hydrophilic, allyldextran/bisacrylamide matrix, 2.6 cm × 60 cm, 320 mL) using elution buffer C consisting of 50 mM Tris-HCl (pH 8.5) and 1 M NaCl at an isocratic flow rate of 1 mL min^{-1}. The most abundant protein peak (fractions 14−20, Figure 1C) was collected, dialyzed, lyophilized, and stored at −20 °C until further use. An ÄKTA Explorer medium pressure chromatography system (Amersham Pharmacia, Uppsala, Sweden) was used for all three chromatographic separations. Protein extract was filtered through a 0.45 μm Whatman GD/X Nylon syringe filter (Whatman Inc., Piscataway, NJ) before being administered into the chromatography system. Elution of protein was monitored as absorbance at 280 nm, and the proteins in each UV absorbing peak were assessed by SDS-PAGE separation.

Protein Identification by Electrophoresis. SDS-PAGE and native-PAGE were carried out using precast minigels (PhastGel gradient 8−25) with PhastGel SDS and native buffer strips (GE Healthcare Life Sciences), respectively. For SDS-PAGE, protein solutions (2 μg protein μL^{-1}) were prepared in 62.5 mM Tris-HCl (pH 6.8) buffer containing 2% (w/v) SDS, 10% (w/v) glycerol, and 0.05% (w/v) bromophenol blue. For native-PAGE, nonreducing buffer (62.5 mM Tris-HCl, pH 6.8 containing 10% (w/v) glycerol) was used. A 1 μL portion of protein solution was loaded onto the precast gel with a PhastGel sample applicator. Electrophoresis was performed at a constant current of 60 mA per gel for approximately 45 min using a PhastGel system. Gels were stained with PhastGel Blue R (Coomassie R 350) stain in 20% (v/v) acetic acid and destained in 1:3:6 acetic acid/methanol/water (v/v/v) solution. The approximate molecular masses (M_r's) of the separated polypeptide bands were determined by comparing with molecular weight standards (6.5−200 kDa, Bio-Rad Laboratories, Hercules, CA) on the same gel.

Microfluidic LabChip Electrophoresis. Purified proteins were analyzed using a microfluidic, chip-based automated electrophoresis system (Experion System, Experion Pro260 starter kit, Bio-Rad Laboratories) under nonreducing conditions. A 4 μL aliquot of protein (2 mg protein/mL in 10 mM Tris-HCl pH 7.4) or Experion Pro260 Ladder was mixed with 2 μL of Experion Pro260 sample buffer containing water, glycerol and lithium dodecyl sulfate and heated at 95 °C for 3−5 min and then diluted with 84 μL of DEPC (diethylpyrocarbonate)-treated water. The protein standard mixture contained β-mercaptoethanol (3.3%, v/v). The protein separation chip was primed with Experion Pro260 Gel containing water, methylurea, and *N*-(2-hydroxy-1,1-bis(hydroxymethyl)ethyl)glycine in the Experion Priming Station. Diluted samples (6 μL) were loaded on to the primed chip and analyzed in the Experion Pro260 electrophoresis station. The subunit molecular weight and their abundance were determined using the position and integral area of fluorescence peaks relative to the Experion Pro260 Ladder proteins.

Protein Measurements. Total nitrogen content of mature seeds was determined by combustion analysis (Flash EA1112 N-analyzer, Thermo Fisher Scientific), and a conversion factor of 5.64 was used to calculate protein content.[15]

Fourier Transform Infrared Spectroscopy (FT-IR). All FT-IR measurements were taken using a Bruker Vertex 70 FT-IR spectrometer (Bruker Optics, Billerica, MA) equipped with a KBr beam splitter in the interferometer and a liquid nitrogen cooled MCT detector. The dry protein powder was mixed with KBr powder (1:125, w/w) using a mortar and pestle and compressed to obtain 13-mm disks. The interferometer was purged with a constant flow of dry nitrogen gas. Each sample was scanned (128 scan), and data acquisition was done at 4 cm^{-1} resolution. Protein secondary structure analysis was carried out using the Opus 6.5 software package (Bruker Optics, Billerica, MA) according to the Fourier self-deconvolution (FSD) method[16] and Gaussian curve-fitting of the amide I region (1610−1700 nm).[17] The percentage of each secondary structure element was calculated from the relative integral area of each fitted curve of the amide I region. Peak assignments of components in the amide I band were as follows: α-helix (1659.1 ± 0.4 cm^{-1}), β-sheet (1616.7 ± 0.4, 1627.8 ± 0.2, 1638.8 ± 0.3, and 1693.3 ± 0.1 cm^{-1}), β-turn (1669.5 ± 0.2 and 1680.9 ± 0.2 cm^{-1}), and random structure (1649.8 ± 0.5 cm^{-1}).[17,18]

Circular Dichroism (CD) Spectroscopy. The far-UV CD spectra of protein solutions (2 mg mL^{-1} in 10 mM sodium phosphate buffer at pH 7.4) were obtained at 25 °C using a PiStar-180 spectrometer (Applied Photophysics Ltd., Leatherhead, U.K.) equipped with a 75 W mercury xenon lamp and 0.1 mm quartz cell and recorded from 180 to 260 nm using a 0.5-nm step size and 6-nm entrance and exit slits. The instrument was calibrated with 0.89 mg mL^{-1} *d*-(+)-10-camphorsulfonic acid. Ten scans per sample were averaged to obtain one spectrum, and the baseline was corrected by subtracting buffer spectra. The mean molar ellipticity $[\theta]$ was calculated using eq 1

$$[\theta](\mathrm{deg\ cm^2\ dmol^{-1}}) = 100(\theta)M/nCl \quad (1)$$

where θ is the measured signal in millidegrees (mdeg), M is the mean residue molecular weight (g mol^{-1}) of the protein (generally assumed to be 115), n is number of amino acid residues of cruciferin protomer, C is the molar concentration (mg cm^{-3}), and l is the path length (cm) of cuvette. Secondary structure of each test protein was estimated using the DicroWeb server (http://dichroweb.cryst.bbk.ac.uk), which employs the CONTIN/LL program with data set 3 and CD spectra of 37 reference proteins.[19]

Zeta Potential. The electrophoretic mobility of proteins in solution was measured as zeta (ζ)-potential with changing pH using a Zetasizer Nano ZS90 (Malvern Instrument Ltd., Westborough, MA) at 25 °C. Protein dispersions (0.05%, w/v) prepared in deionized water and filtered through a 0.45 μm Whatman GD/X Nylon syringe filter (Whatman Inc., Piscataway, NJ) were titrated from pH 10 to 2 (by 0.5 units) in a 1.5 mL disposable folded capillary cell using a Zetasizer equipped with a multipurpose MPT-2 autotitrator (Malvern Instrument Ltd., Westborough, MA) with 0.5 M and/or 0.005 M HCl or 0.01 M NaOH. The pH value of zero ζ-potential was considered as the isoelectric point (p*I*) of the protein.

Intrinsic Fluorescence. The fluorescence emission spectra of protein in solution (50 μg mL^{-1} in 10 mM Tris-HCl buffer, pH 7.4, 20 °C) were recorded with a FluoroMax-4 spectrofluorometer (Horiba Jobin Yvon, Edison, NJ) with the excitation wavelength at 280 nm and emission scanned from 290 to 430 nm (5 nm excitation and emission bandwidth).

Acrylamide was used as an aqueous nonionic quencher to characterize the microenvironment of Trp residues. The fluorescence intensity of protein (800 μL of 50 μg mL^{-1}) upon addition of 10 μL aliquots of 5 M acrylamide solution was taken as described above. The classical Stern−Volmer eq 2 that describes the relationship between fluorescence intensity and quencher concentration for a dynamic bimolecular collisional quenching system[20] was employed to calculate the Stern−Volmer constant K_{sv} of each protein

$$F_0/F = 1 + K_{sv}[Q] \quad (2)$$

where F_0, F, $[Q]$, and K_{sv} are initial fluorescence intensity without quencher, the fluorescence intensity of a given quencher concentration, quencher concentration, and the Stern−Volmer constant, respectively.

The modified Stern−Volmer eq 3 was used for calculating the association constant K_a

$$F_0/(F - F_0) = 1/f_a K_a[Q] + 1/f_a \quad (3)$$

where f_a is the fractional accessibility of fluorophores, and K_a is the association constant.

Protein solution (50 μg mL^{-1}) spectra were obtained with the addition of 6 M urea or 6 M guanidine-HCl and by changing the pH from 2 to 10.

ANS Binding. Binding of 1-anilino-8-napthalensulfonate (ANS) to the protein was used as a measure of surface hydrophobicity (S_0) according to the modified method of Kato and Nakai.[21] ANS (10 μL of 8 mM stock solution) was added to 800 μL of protein solution (0.05−0.25 mg mL^{-1} in 10 mM phosphate buffer, pH 7.4), and incubated for 5 min in the dark, followed by fluorescence emission scanning between 425−465 nm (excitation 390 nm, slit widths 5 nm). The S_0 value (an index without units) was determined from the initial slope of the linear regression line fitted for the measured fluorescence intensity against protein concentration (mg mL^{-1}). Binding of ANS was evaluated at 23, 50, 70, and 90 °C with the temperature of the protein solutions (50 μg mL^{-1}) being maintained using a Peltier temperature controller (model LFI-3751, Wavelength Electronics Inc., Bozeman, MT).

Thermal Properties. Thermal denaturation parameters of proteins were obtained using a TA Q2000 differential scanning calorimeter (DSC) equipped with Plantinum software (TA Instruments, New Castle, DE). Approximately 10 mg of 10% (w/v) protein slurry in 10 mM phosphate buffer (pH 7.4) was placed into aluminum liquid pans, hermetically sealed with Tzero press (TA Instruments, New Castle, DE), and subjected to 30 to 130 °C at a scanning rate of 10 °C min^{-1} under constant nitrogen purging (flow 50 mL min^{-1}). A hermetically sealed empty pan was used as a reference. Denaturation temperature (T_m), width at half peak height ($\Delta T_{1/2}$), experimental enthalpy change ($\Delta H_{exp Tm}$), and heat capacity change ($\Delta C_{pN\rightarrow U}$) upon protein unfolding were computed from thermograms using the Universal Analysis 2000, version 4.7A software (TA Instruments-Water LLC). The calorimetric van't Hoff enthalpy change (ΔH_{vHTm}) for an oligomeric protein with n monomers, which is 12 for 11S globulins,[22] was calculated using eq 4[23]

$$\Delta H_{vHTm} = [(\sqrt{n} + 1)^2 RT_m^2 C_{pmax}]/\Delta H_{exp\ Tm} \quad (4)$$

where R is the gas constant 8.314 51 J K^{-1} mol^{-1} and C_{pmax} is the maximum heat capacity at denaturation.

The Gibbs free energy of unfolding of protein can be written as eq 5

$$\Delta G_{Tm} = -RT \ln K_{eqN\leftrightarrow U} = \Delta H_{exp\ Tm} - T_m \Delta S_{Tm} \quad (5)$$

dx.doi.org/10.1021/jf400559x | J. Agric. Food Chem. 2013, 61, 5848−5859

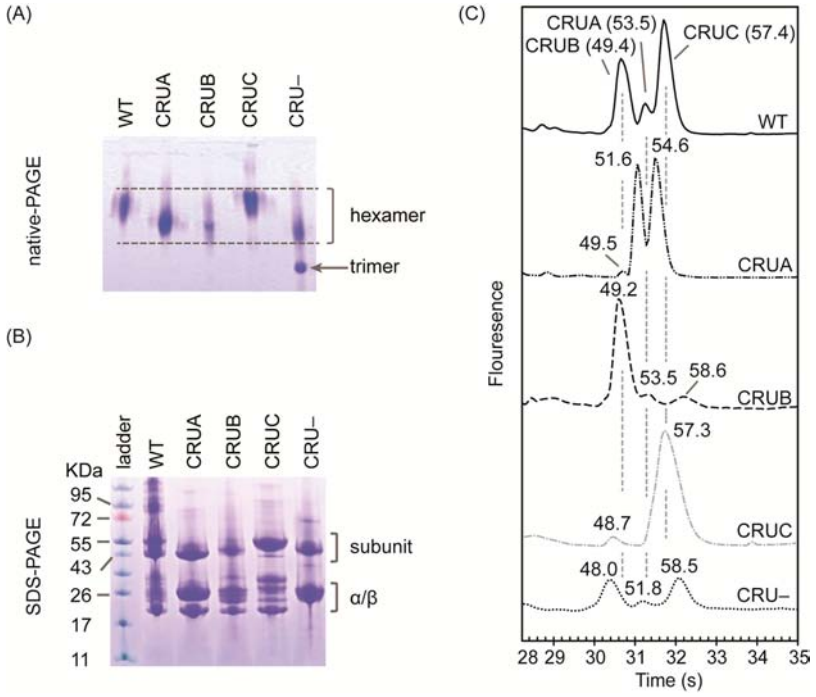

Figure 2. Electrophoretic separation of isolated cruciferin from *Arabidopsis*. (A) Native-PAGE showing separation of cruciferins under nondissociating conditions. All have hexameric form except the triple-knockout, CRU-. (B) SDS-PAGE of purified cruciferin under nonreducing conditions showing intact S−S bonds in the subunits (α−S−S−β) and free α- and β-chains. (C) LabChip microfluidic electrophoretic profiles of purified cruciferins under nonreducing conditions showing estimated molecular weights (kDa) of each cruciferin subunit.

where $K_{eqN\leftrightarrow U}$ is the equilibrium constant, which is equal to 1 at T_m when native and unfolded state populations are equal. Therefore, entropy change upon denaturation (ΔS_{Tm}) can be obtained from eq 6:

$$\Delta S_{Tm} = \Delta H_{exp\ Tm}/T_m \quad (6)$$

Statistical Analysis. All studies were carried out in triplicate. The data analysis was a one-way analysis of variance (ANOVA) using the General Linear Model (GLM) procedure of SAS Version 9.1 (SAS Institute Inc. Cary, NC).[24] Mean separation was carried out, and the least significant difference (LSD) was calculated when the main effect was significant ($P < 0.05$, $P < 01$, or $P < 0.001$).

RESULTS AND DISCUSSION

The *Arabidopsis* cruciferin genes AT5G44120.3, AT1G03880.1, and AT4G28520.1 encode the CRUA, CRUB, and CRUC cruciferin protomer (subunit) variants, respectively. These protomers randomly assemble as a heterohexamer and form the quaternary structure of WT cruciferin. The cruciferin mutant lines produce 11S protein composed of a single subunit type either CRUA, CRUB, or CRUC (double-knockout lines). A triple-knockout line that does not express any of the cruciferin genes (*CRU-*) was also generated.

Purification of Cruciferin from WT and Mutant Lines. The chromatographic separation and purification steps described by Bérot et al.[12] and successfully applied to obtain cruciferin from other crucifer oilseeds[13] were used to purify *Arabidopsis* cruciferin (Figure 1). The first size exclusion chromatographic (SEC, Sephadex G-25) step excluded protein (cruciferin, napin, and other proteins) in the void volume (Figure 1A) and separated them from UV-absorbing phenolic compounds (Figure 1A). Further separation of the SEC protein peak by CEC resulted in elution of crude cruciferin in the unbound peak (Figure 1B). Napin remained bound to the CEC column and can be released later by increasing NaCl concentration.[12] The last SEC separation resolved four protein peaks in which the predominant protein peak II contained cruciferin subunit bands of 50−55 kDa, while peak I had very little native cruciferin and peaks III and IV contained small molecular weight polypeptides of ∼13 kDa (Figure 1C inset). Comparison of SEC profiles of all cruciferin types (Figure 1D) indicated that the triple-knockout line may contain a very low amount of cruciferin-like proteins. Although the plants of triple-knockout line do not express cruciferin genes, seed N content based on protein level remained comparable with WT,[11] possibly due to accumulation of noncruciferin proteins, polypeptides, or free amino acids to compensate for the loss of cruciferin, similar to that reported in barley and soybean.[25,26] Proteins obtained from this process were >95% pure.

Cruciferin Subunit Composition. According to native-PAGE, undissociated CRUA, CRUB, CRUC, and WT cruciferin had one type of native protein assembly. The *CRU-* line had two types of native protein assemblies that migrated separately (Figure 2A). Western blot analysis with an anticruciferin antiserum demonstrated that the complexes in the *CRU-* line are not cruciferin.[11] This was confirmed by transcriptomic and proteomic analysis that revealed an increase in *cupin* domain proteins similar to the trimeric 7S globulins which appear to compensate for the loss of cruciferin in this line (unpublished data). The calculated M_r values of CRUA, CRUB, and CRUC subunits based on amino acid sequence were 52.6, 50.6, and 58.2 kDa, respectively.[10] Accordingly, each of the mutant lines appears to have produced a cruciferin complex with six subunits having hexameric native conformation (ca. M_r 303−350 kDa). One of the MW complexes seen in the *CRU-* line, which may be a 7S globulin trimer, is not seen in the double-knockout lines, further indicating that these complexes consist of single subunits.

dx.doi.org/10.1021/jf400559x | J. Agric. Food Chem. 2013, 61, 5848−5859

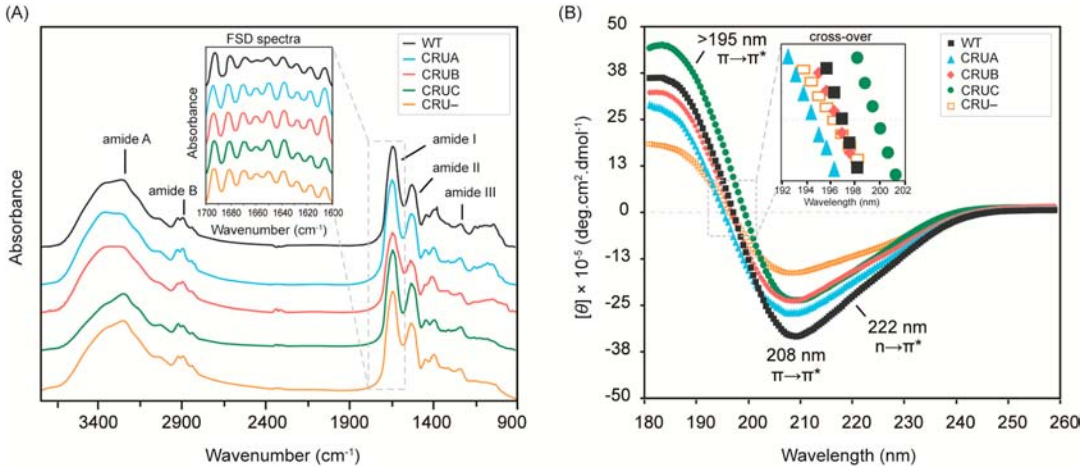

Figure 3. Secondary structure analysis of purified cruciferins. (A) FT-IR spectra of purified cruciferins showing the amide A, B, I–III peaks. Inset shows secondary structure components within the amide I peak (1650 cm^{-1}) resolved by FSD. (B) Far-UV CD spectra of cruciferins (pH 7.4) from 180 to 260 nm showing $\alpha + \beta$ type characteristics: a broad negative band at around 208 nm, a positive peak in the 195–180 nm region, and a negative to positive crossover point at around 200 nm. $[\theta]$ is the mean residue ellipticity.

SDS-PAGE revealed polypeptides in the molecular mass range 45–60 kDa (Figures 1C, inset, and 2B) with intact disulfide bonds between the α- and β-chains (α–S–S–β). The absence of protein bands of <20 kDa indicated no contamination of napin in the purified proteins.[13] The polypeptide bands of ~20 and ~30 kDa for WT and double-knockout lines are free cruciferin α- and β-chains that arise due to disulfide interchange that occurs during protein sample preparation as observed in *A. thaliana*, *B. napus*, and *R. sativus*,[27] or during intracellular transport.[28]

The three peaks identified in WT cruciferin by LabChip microfluidic electrophoresis were estimated to have molecular masses (M_r's) of 53.5, 49.4, and 57.4 kDa which can be assigned as CRUA, CRUB, and CRUC, respectively (Figure 2C). These values are very close to the calculated M_r values of CRUA (52.6 kDa), CRUB (50.6 kDa), and CRUC (58.2 kDa) based on their primary sequences.[10] The relative abundance of CRUA, CRUB, and CRUC subunits in WT cruciferin based on the fluorescence peak area was 9.6% (72.8 ng μL^{-1}), 32.8% (249.5 ng μL^{-1}), and 57.6% (438.5 ng μL^{-1}), respectively, and in an approximate ratio of 1:3:6 for CRUA:CRUB:CRUC subunits. On the basis of sequence coverage obtained from MS analysis, CRUC (AT4G28520.1) is the major cruciferin isoform contributing to total seed protein of *A. thaliana* (cv. Columbia).[29] The CRUA double-knockout line showed two partially resolved peaks at 51.6 and 54.6 kDa that gave an average value of 53.1 kDa, which matches with the CRUA peak of WT (Figure 2C). This type of partial resolution of protein peaks has been reported for *Arabidopsis* and pea 11S globulins resulting from disulfide interchange with free –SH groups during sample preparation in SDS-PAGE buffer as described by Rödin and Rask[28] and Inquello et al.[27] or upon thermal processing.[30] The LabChip microfluidic sample buffer contains lithium dodecyl sulfate which may support disulfide–SH exchange similar to SDS when protein is heated at 95 °C for 2–3 min. Examination of molecular structure of cruciferin shows that CRUA and CRUB have free –SH groups in the proximity (9.3 Å apart) of the interchain disulfide bond at Cys293 and Cys280, respectively (Supporting Information, Figure S1), whereas CRUC has no free accessible –SH group close to interchain disulfide bond (Supporting Information, Figure S2).[10] In the CRUB structure, the relatively long side chain of Thr277 and Met278 residues between the free –SH groups and interchain disulfide bond may pose a substantial barrier to disulfide–SH exchange reaction (Supporting Information, Figure S1). However, in CRUA, there is no such steric interference with the corresponding amino acids; the short side chains of Ser290 and Ala291 would allow CRUA to undergo intramolecular sulfhydryl–disulfide exchange reaction. The major peaks of homomeric CRUB and CRUC have values of 49.2 and 57.3 kDa, which are fairly close to the corresponding subunits of WT *Arabidopsis* (Figure 2C). The CRU- protein gave three faint peaks at 48.0, 51.8, and 58.5 kDa that did not correspond to cruciferin subunit.

Secondary Structure Components of Cruciferin. FT-IR spectra of pure cruciferins revealed five amide bands: amide A (100% νN—H) at 3302–3307 cm^{-1}, amide B (100% δN—H) at 2931–2933 cm^{-1}, amide I (80% νC═O, 10% νC—N) at 1652–1653 cm^{-1}, amide II (60% δN—H, 40% νC—N) at 1536–1540 cm^{-1}, and amide III (40% νC—N, 30% δN—H, δC═O) at 1238–1241 cm^{-1} (Figure 3A), which were identified according to Miyazawa et al.[31] and Susi.[32] The strongest amide I band was used for FSD to calculate secondary structure components (Table 1).

All of the cruciferin CD spectra (Figure 3B) had a broad negative peak at about 208 nm ($\pi \rightarrow \pi^*$) and a positive peak in the 180–195 nm ($\pi \rightarrow \pi^*$) region; the crossover point from negative to positive was at 200 nm, which is typical for an "$\alpha + \beta$ type" protein.[33] The characteristic negative band at 222 nm ($n \rightarrow \pi^*$) from α-helices[33] was not observed, in accordance with the less predominant α-helical structure of cruciferin. Similar CD spectra were reported for native rapeseed cruciferin[34] (84% pure) and soy glycinin[35] (~90% pure).

Both FSD of the FT-IR amide I (1610–1700 nm) band and CD analysis showed predominant β-sheet content. The α-helix content of CRUA, CRUB, and CRUC was less than the contents of turn or random structure (Table 1). The predominant β-sheet content confirms previous reports on cruciferin secondary structure.[1,10] The random structure content of these cruciferins determined from CD spectra (25.2–26.2%) was different compared to that from FSD FT-IR (13.6–16.4%). Among the homohexamers, FT-IR data from

dx.doi.org/10.1021/jf400559x | J. Agric. Food Chem. 2013, 61, 5848–5859

Table 1. Secondary Structure Features (%) of Purified Cruciferins from Arabidopsis

protein	α-helix	β-sheet	turn	random
Secondary Structures from FSD Analysis of FT-IR Amide I				
WT	9.2[b]	44.1[d]	35.1[a]	11.6[e]
CRUA	8.3[c]	47.9[b]	28.9[c]	14.9[c]
CRUB	8.9[b]	50.3[a]	27.2[d]	13.6[d]
CRUC	7.2[d]	46.6[c]	29.9[b]	16.4[b]
CRU-	14.2[a]	39.9[e]	26.7[d]	19.2[a]
s.e.m.	0.35	0.51	0.44	0.38
Secondary Structures from Far-UV CD Spectra				
WT	7.9[b]	44.6[a]	22.0[a]	25.6[a]
CRUA	7.4[b]	43.8[a]	22.9[a]	26.2[a]
CRUB	7.7[b]	44.6[a]	21.5[a]	26.1[a]
CRUC	7.8[b]	45.3[a]	21.9[a]	25.2[ab]
CRU-	21.1[a]	27.9[b]	28.8[b]	22.4[b]
s.e.m.	1.79	1.90	0.98	0.54
Secondary Structures from Homology Models[a]				
CRUA	12.6	33.8	43.6	10.0
CRUB	13.0	32.3	48.7	6.0
CRUC	12.4	28.8	38.8	20.0

[a]Theoretical values were calculated as percentage of the number of residues in corresponding secondary structure to the total residues in the subunit.[10] Means followed by the same letter within a column of the same data set do not differ significantly ($P < 0.05$); s.e.m. represents standard error of the mean. Assays were conducted in triplicate.

CRUC showed lower α-helix and β-sheet contents and higher contents of turns and random structure than CRUA or CRUB (Table 1). According to homology modeling,[10] the long hypervariable region of CRUC (HVR-I, 60 residues) causes the higher degree of random structure in CRUC, and this was confirmed by FT-IR data (Table 1). The lower ($P < 0.05$) β-sheet content (39.9% from FT-IR and 27.9% from CD) and higher α-helix content (14.2% from FT-IR and 21.1% from CD) of the proteins remaining in the *CRU-* line, in combination with electrophoresis data, indicate that the compensatory proteins in the *CRU-* line are different from cruciferins.

Electrical Potential of Cruciferins. The protein surfaces in an aqueous medium are naturally charged to form an electrical double layer, and the ζ-potential is the potential at the boundary of this layer (surface of hydrodynamic shear). The ζ-potential value of all cruciferins changed from negative to positive when pH was reduced from 10 to 2.0 (Figure 4). The proteins exhibited a high potential stability in the pH range 7.0−10 as the ζ-potential remained between −57 and −17 mV (we consider −30 mV as the dividing value between stable and unstable colloidal systems). The ζ-potential of CRUB remained well below −30 mV in the basic to neutral pH range with minor fluctuations. In contrast, the CRUC homohexamer, which showed the highest negative potential of −55 mV at pH 9.0, exhibited rapid change in ζ-potential when the pH approached neutrality. At acidic pH (3.4 to 4.9) all proteins, except CRUC homohexamer, showed zero ζ-potential. During the titration of protein from pH 7.0 to 3.0, the ζ-potential of all cruciferins moved to a positive value with a high +28.0 mV for CRUC and +5.0 to +10.0 mV for CRUA, CRUB, and the WT heterohexamer. The change of ζ-potential beyond pH 3.0 was not drastic and approached zero when at a pH of 2.0. The differences in ζ-potential change observed for CRUA, CRUB, and CRUC homohexamers indicated differences in the charges of their surface residues. According to homology models for these three cruciferins,[10] the IA face (solvent exposed) of CRUC showed higher electronegativity that was spread more evenly over the entire surface area than CRUA or CRUB, confirming the observation made on ζ-potential change as a

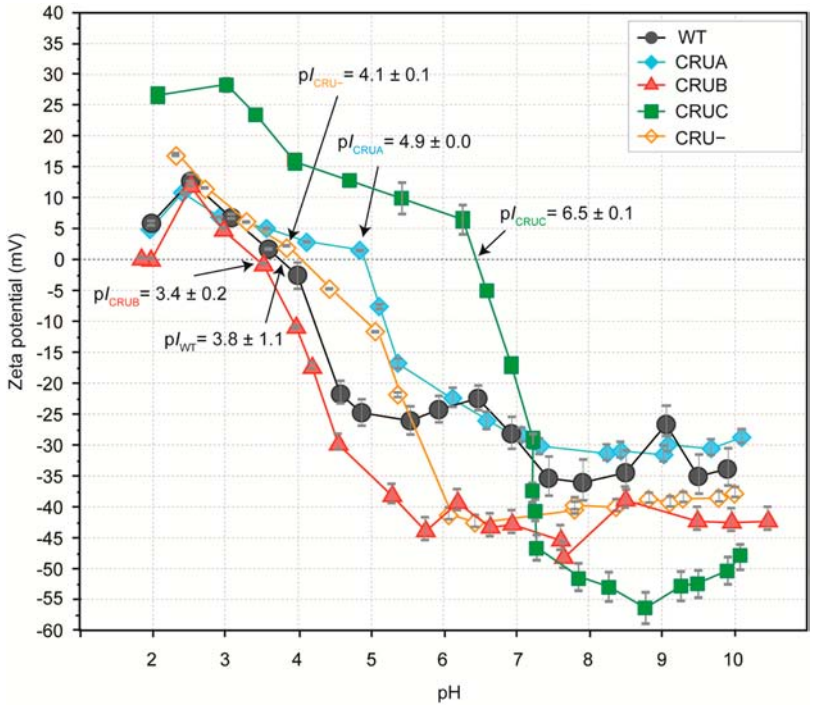

Figure 4. Zeta (ζ) potential of cruciferins (0.1 mg mL^{-1}) at different pH values. The locations and values of the isoelectric points (p*I*) where ζ = 0 are indicated. Error bars denote ±sd of triplicate measurements.

dx.doi.org/10.1021/jf400559x | J. Agric. Food Chem. 2013, 61, 5848−5859

function of pH. The surface charge of these three cruciferins at pH ~ 7.4 is comparable with the ratio of acidic and basic amino acids CRUC (3.2:1) > CRUB (2.5:1) > CRUA (2.0:1) calculated on the basis of primary sequences. When the proteins were titrated beyond the neutral pH to acidic pH, all cruciferins passed through a point where ζ-potential becomes zero. The zero net charge or isoelectric point (p*I*) for CRUA, CRUB, CRUC, and WT cruciferins was at pH 4.9, 3.4, 6.5, and 3.8, respectively. The p*I* values calculated on the basis of the amino acid composition of the subunits are 7.68 for CRUA, 6.53 for CRUB, and 6.53 for CRUC. Except for CRUC, the pH value of zero ζ-potential was far different than the calculated value. No reports are available on experimental p*I* values for *Arabidopsis* or *B. napus* cruciferin. The p*I* value derived from the pH dependent solubility curve (minimum solubility at its p*I*) for procruciferin Cru2/3a was at pH ~ 4.2 (μ = 0.08),[6] and the calculated value based on amino acid composition was pH 6.6,[10] indicating that theoretical values do not always agree with observed values. The conformation of the protein in solution affects the extent of residues available for ionization, which in turn reflects charge neutralization by H ions as the pH changes. As such, the three-dimensional structure can cause a considerable difference between calculated and experimental p*I* values for native proteins.[36] Among the cruciferins studied, the pattern of ζ-potential as a function of pH indicated that CRUC has more ionizable residues on the solvent accessible surface than do the other cruciferins. The net electrical charge of a protein under given solvent environment strongly affects their physicochemical properties and, therefore, the functionalities they provide.

Intrinsic Tryptophan Fluorescence. Intrinsic fluorescence due to the indole ring of tryptophan depends on the polarity of the surrounding microenvironment.[37] The number of Trp residues in the primary sequence of the cruciferin variants was considerably different, CRUA with 30, CRUB with 36, and CRUC with 54 (Table 2). However, only slight differences in the steady-state fluorescence emission or peak area were observed (Figure 5A), indicating a comparatively lower number of solvent-exposed Trp residues in CRUC than in CRUA. CRUA had the lowest λ_{max} (333 nm) among the cruciferins (Table 2) suggesting that a more hydrophobic environment exists around the Trp indole moieties than in the other cruciferins, possibly buried in hydrophobic pockets.[38] The very low fluorescence intensity and the extremely red-shifted λ_{max} emission band of 351 nm (Table 2) observed for CRU- protein (~13 nm from *Arabidopsis* WT cruciferin) suggested that its Trp residues have greater solvent accessibility and, therefore, possibility of solvent-induced fluorescence quenching.

Acrylamide, a nonionic neutral quencher, decreases fluorescence emission intensity from Trp residues when it binds to or is in the proximity of a fluorophore. The increase in quencher concentration attenuated fluorescence emission intensity of all cruciferins (Figure 5B) and shifted λ_{max} to lower wavelengths (i.e., hypsochromic shift) (Figure 5B, inset). The nonlinear Stern–Volmer plots (Figure 5C) for all cruciferins exhibited an upward concave curvature toward the *y*-axis, especially at high acrylamide concentrations, indicating that the proteins exhibited both static and dynamic quenching processes (static via formation of a ground state fluorophore–quencher complex and dynamic via collision between fluorophore and quencher molecules).[39] Fluorescence quenching at low acrylamide concentrations up to ~0.4 M exhibited a linear (r^2 > 0.99) relationship in the Stern–Volmer plots (Figure 5C, inset), allowing the Stern–Volmer constant (K_{sv}) to be calculated for each protein (Table 2). The low K_{sv} value for the CRUC homohexamer (6.23 M^{-1}) indicated less exposed Trp residues compared to the other cruciferin variants; therefore, the residues may be buried inside the structure. A less compact protein molecule may allow greater exposure of its fluorophores to the environment than a more compact molecule; therefore, the low K_{sv} may indirectly indicate a high degree of molecule compactness. The CRU- protein had the highest K_{sv} value (P < 0.05) of 15.25 M^{-1}, indicating a less compact molecule and solvent exposed Trp residues in the structure. The $K_{sv.}$ of CRUB (8.81 M^{-1}) and the WT cruciferin (9.12 M^{-1}) also indicated less compact molecules compared to the CRUA or CRUC homohexamers. The modified Stern–Volmer plots[40] for cruciferins were linear (Figure 5D) indicating possible static quenching of heterogeneous Trp residues in cruciferins. Association constants (K_a) calculated using the modified Stern–Volmer plots (Table 2) were the lowest (3.91 M) for the CRUC homohexamer (Figure 5D), further suggesting that the Trp residues may be buried within hydrophobic regions (i.e., interchain disulfide containing face, IE face) of the hexamer and may be shielded from solvent. Such residues may undergo quenching by an aqueous agent when the hexamer is dissociated. Similar to the K_{sv} values, the highest K_a value of 13.62 M was observed for CRU- which further confirmed a more relaxed structure for this protein. The association constant of the CRUA homohexamer did not differ significantly (P > 0.05) from that of CRUB, but was lower (P < 0.05) than the WT heterohexamer (Table 2).

Table 2. Various Fluorescence Parameters Oobtained from Intrinsic Fluorescence and Probe Binding Methods[a]

		from intrinsic fluorescence			
protein	no. of Trp residues from calculation[b]	λ_{max} (nm)	K_{sv} (M^{-1})	K_a (M)	from ANS probe florescence S_o
WT		338 ± 0.0	9.12[b]	6.91[b]	446.4[b]
CRUA	30	333 ± 0.5	7.00[c]	5.20[c]	525.3[a]
CRUB	36	345 ± 0.5	8.81[b]	5.43[c]	444.5[b]
CRUC	54	340 ± 0.0	6.23[d]	3.91[d]	282.1[c]
CRUC-		351 ± 1.0	15.25[a]	1362[a]	236.7[d]
s.e.m.			1.05	1.15	36.4

[a]K_{sv}: Stern–Volmer quenching constant. K_a: Stern–Volmer association constant. S_o: surface hydrophobicity. [b]Calculated from the homotrimers.[10] Means followed by the same letter within a column do not differ significantly (P < 0.05). s.e.m. standard error of the mean. Means followed by the same letter within a column do not differ significantly (P < 0.05). Assays were conducted in triplicate.

Structural Stability in the Presence of the Cosolvents Urea, Guandine-HCl, and NaCl or in Response to pH Change. The changes that occur in the Trp environment due to small organic molecules, such as urea and guanidine-HCl, can be followed by measuring intrinsic fluorescence (Figure 6) to provide information on protein structure stability. With the exception of CRUC homohexamer, the other homohexamers and WT cruciferin showed a λ_{max} red shift (Figure 6A,C) with a concomitant increase in fluorescence intensity in urea treated samples (Figure 6B). This indicates that urea caused unfolding to expose Trp residues. Guanidine-HCl caused a drastic decrease (<50%) in fluorescence yield for all cruciferins other

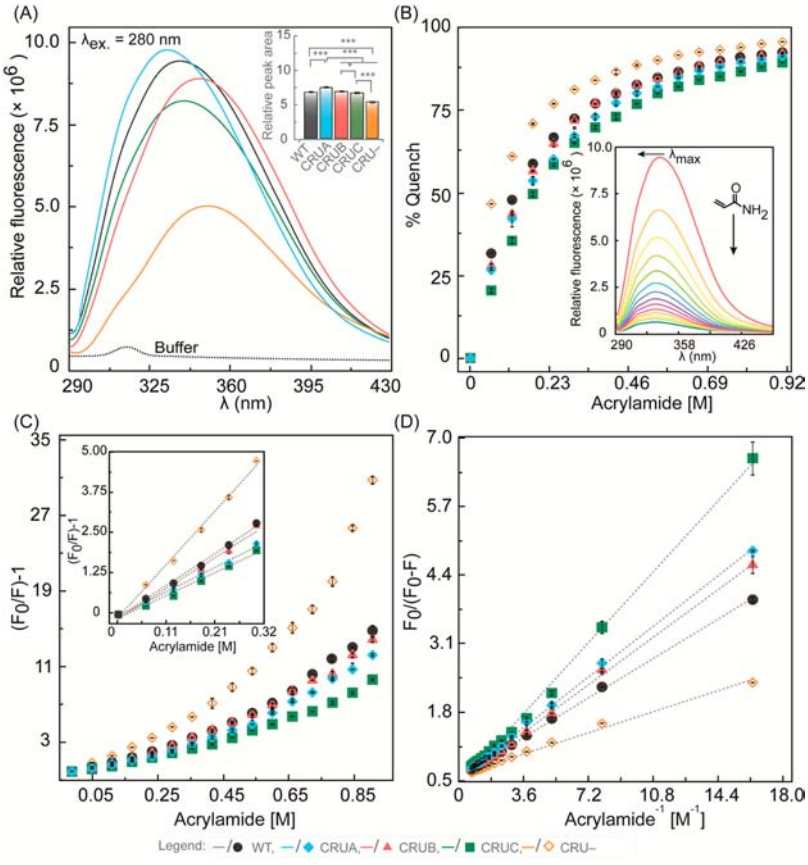

Figure 5. Intrinsic fluorescence of cruciferin and fluorescence quenching due to acrylamide. (A) Fluorescence emission spectra for hexameric cruciferins. (B) Primary plot of fluorescence quenching as a function of acrylamide (C_3H_5NO) concentration. Inset shows quenching of cruciferin from WT *Arabidopsis* with the addition of acrylamide. (C) Stern–Volmer plots exhibiting positive deviation from linearity. Inset shows Stern–Volmer plots showing linear relationships ($r^2 > 0.99$) at low quencher concentrations that were used to calculate Stern–Volmer quenching constant (K_{sv}). (D) Linearity of the modified Stern–Volmer plot indicating static quenching of different accessible populations of fluorophores (i.e., buried and exposed tryptophan residues). The plots allowed calculation of the Stern–Volmer association constant (K_a) of exposed tryptophan residues (values are shown in Table 2). All measurements were taken at 50 μg mL^{-1} protein in 10 mM phosphate buffer at pH 7.4, excitation was at 280 nm.

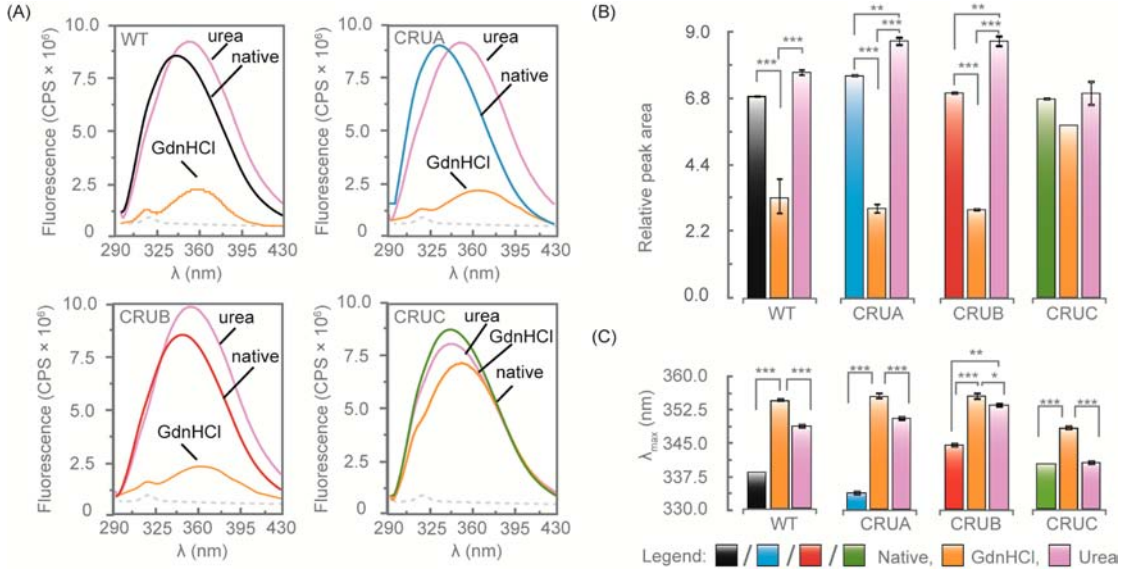

Figure 6. Tryptophan fluorescence of native cruciferins and denaturation induced by 6 M urea and 6 M guanidine-HCl. (A) Fluorescence emission spectra, (B) peak area, and (C) emission maximum (λ_{max}). All spectra were recorded at an excitation wavelength of 280 nm. *$P < 0.05$, **$P < 0.01$, ***$P < 0.001$.

dx.doi.org/10.1021/jf400559x | J. Agric. Food Chem. 2013, 61, 5848–5859

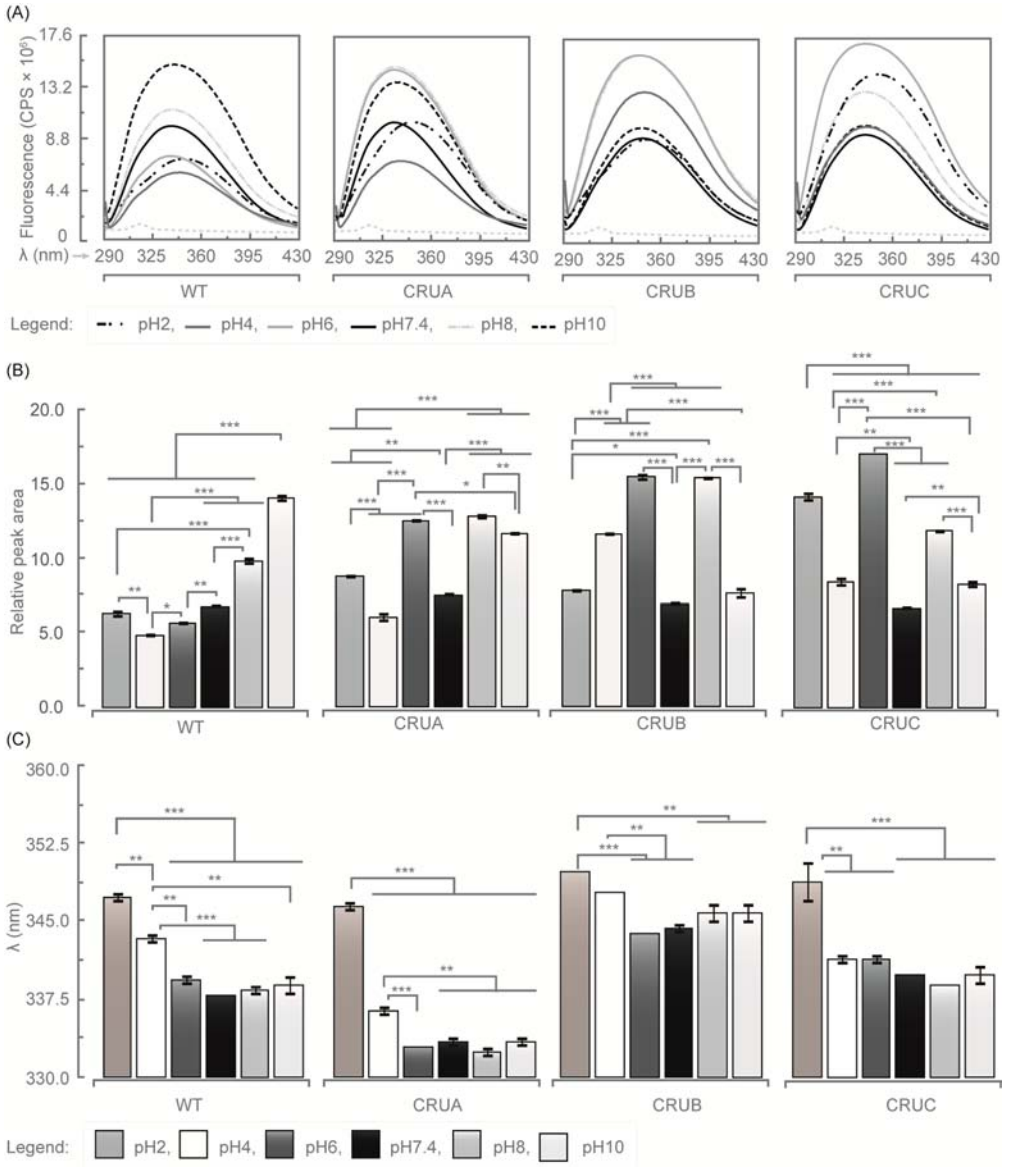

Figure 7. Intrinsic fluorescence of cruciferin as a function of pH: (A) emission spectra, (B) fluorescence peak area, (C) maximum wavelength of emission. All spectra were recorded at an excitation wavelength of 280 nm. *$P < 0.05$, **$P < 0.01$, ***$P < 0.001$ (ANOVA). Error bars, ±sd ($n = 3$).

than CRUC. Of all the cruciferins (Figure 6A,B), fluorescence emission intensity of the CRUC homohexamer remained fairly similar to its native state in the presence of both chaotropic agents, and the λ_{max} value remained unchanged with 6 M urea, suggesting that either complete opening of the CRUC homohexamer does not occur easily or that intramolecular and solvent-induced quenching of Trp residues happens upon exposure to these agents.

Sodium chloride can stabilize protein structure when present as a cosolvent, but this is dependent on its concentration. The presence of NaCl at concentrations ranging from 0.2 to 1.0 M had a negligible effect on λ_{max}. Except for CRUA, the WT, CRUB, and CRUC showed an increase in fluorescence intensity and peak area with NaCl, but there was no difference among different concentrations (Supporting Information, Figure S3). This indicates that the presence of NaCl up to 1.0 M causes minimal disturbance in the structural stability of these cruciferins at pH 7.4.

The λ_{max} value showed a red shift for all cruciferins when pH reduced from neutral to acidic (Figure 7), which increased when the ionic strength was brought up to 0.5 at pH 7.4 (data not shown). As the pH was lowered from neutral, the fluorescence intensity initially increased and then decreased for cruciferin (except WT), indicating possible exposure or change of the hydrophobic environment of Trp residues around pH 2.0. Continued increase in fluorescence intensity and λ_{max} for CRUC when pH is as low as 2.0 indicated that an opposite sequence of events may be occurring. Marcone and co-workers[41] showed that red shift and decrease in fluorescence intensities under acidic conditions for globulin proteins are due to exposure of one or more hydrophobic surfaces, while maintaining secondary structure. It is possible that at pH 2.0 the cruciferin hexamers dissociate, exposing the IE face of the trimers making Trp residues more accessible to the solvent. Increasing the pH to alkaline (up to 10) caused only a minor bathochromic or hypsochromic shift of the emission spectra for

Table 3. Differential Scanning Calorimetric (DSC) Thermal Properties[a] of the Cruciferin Proteins

protein	T_m (°C)	$\Delta T_{1/2}$ (°C)	$\Delta C_{pN\rightarrow U}$ (kJ K^{-1} mol^{-1})	ΔS_{Tm} (kJ K^{-1} mol^{-1})	ΔH_{expTm} (kJ mol^{-1})	ΔH_{vHTm} (kJ mol^{-1})	$\Delta H_{expTm}/\Delta H_{vHTm}$
WT	100.2^{c}	6.9^{a}	0.49^{a}	0.44^{b}	166.7^{b}	158.6^{ab}	0.96 ± 0.18
CRUA	100.2^{c}	5.7 ^{c}	0.51^{a}	0.37^{c}	137.2^{c}	139.9^{b}	1.03 ± 0.09
CRUB	102.1^{bc}	6.0^{bc}	0.46^{a}	0.32^{d}	123.3^{d}	128.3^{b}	1.04 ± 0.12
CRUC	113.5^{a}	5.0^{d}	0.36^{ab}	0.47^{a}	181.6^{a}	189.2^{a}	1.04 ± 0.15
CRU-	100.6^{c}	6.3^{b}	0.22^{b}	0.26^{e}	102.8^{e}	16.0^{c}	0.16 ± 0.02
s.e.m.	1.4	0.2	0.04	0.02	7.7	16.3	

[a]Denaturation temperature, T_m; width at half peak height, $\Delta T_{1/2}$; heat capacity change, $\Delta C_{pN\rightarrow U}$; entropy change, ΔS_{Tm}; ΔH_{expTm}, experimental enthalpy change; ΔH_{vHTm}, van't Hoff enthalpy upon unfolding. Means followed by the same letter within a column do not differ significantly ($P < 0.05$). s.e.m. indicates standard error of the mean. Assays were conducted in triplicate.

all cruciferins, indicating that little conformational alteration is occurring in response to increasing pH.

Surface Hydrophobicity. Among the cruciferins, heterohexameric WT and homohexameric CRUB gave similar S_0 values, indicating comparable prevalence of ANS anion binding hydrophobic areas exposed to the solvent environment. CRUA showed the highest surface hydrophobicity of S_0 = 525.3 (Table 2). The lowest S_0 value among homohexamers was for CRUC (282.1) which may be related to the lowest number of solvent exposed hydrophobic residues (57 in CRUA, 64 in CRUB, and 31 in CRUC) on the IA face.[10]

In addition, the net negative charge on the CRUC IA face as observed by its ζ-potential (−42 mV at pH 7.4) (Figure 4) may repulse the anionic ANS molecular probe resulting in further inhibition of ANS binding.[42] When CRUA and CRUB S_0 values are compared, the ζ-potential at pH 7.4 and number of solvent exposed hydrophobic residues together explain the higher value for CRUA than that for CRUB homohexamer, indicating that the electrostatic charge on the molecule surface may be responsible for the difference in the observed S_0 values and theoretical number of accessible hydrophobic residues. Increasing the temperature of the protein solution beyond 70 °C caused an increase in cruciferin surface hydrophobicity with a more substantial change for CRUA and WT. For CRUC, an increase in temperature to 90 °C is not expected to cause a high degree of unfolding or reveal more ANS binding sites (Supporting Information, Figure S4).

Thermal Transitions and Stability. The denaturation temperature of the cruciferin variants ranged from 100.2 to 113.5 °C. CRUC homohexamer exhibited the most thermostable structure having a 10−13° higher T_m value (113.5 °C) than WT heterohexamer or other two homohexamers (Table 3, Supporting Information, Figure S4). The proteins in the *CRU-* line had a T_m value of 100.6 °C. The thermal stability of a protein in aqueous system is the net free-energy change ($\Delta G_{N\rightarrow U}$) due to hydrophobic interactions ($\Delta G_{H\Phi}$) and the difference in conformational entropy (ΔG_{conf}) upon heat denaturation ($\Delta G_{N\rightarrow U} = \Delta G_{H\Phi} + \Delta G_{conf}$).[43] During hexamer formation, cruciferin trimers interact through hydrophobic residues.[1] In the CRUC homohexamer, the trimer IE face contains HVR-I and HVR-II which together compose the highest number of hydrophobic residues among the cruciferin variants. This would provide strong interaction between the two trimers and contribute to the high T_m value. Decrease in protein stability due to sulfhydryl (−SH)−disulfide (S−S) interchange during thermal treatment has been reported.[30,43] As discussed earlier, CRUA is more prone to SH−SS interchange than CRUB in which access to the Cys residues is sterically hindered by Thr277 and Met278 (Supporting Information, Figure S1), but CRUC has no free −SH group in the vicinity to exchange.[10] All these may contribute to the observed differences in T_m values among the three cruciferin homomeric variants which were in the decreasing order of CRUA < CRUB < CRUC.

Protein thermal denaturation is a highly cooperative process, and the sharpness of the thermal transition peak (width at half peak height, $\Delta T_{1/2}$) is a measure of cooperativeness; a low $\Delta T_{1/2}$ value indicates a highly cooperative unfolding process.[44] The $\Delta T_{1/2}$ obtained for CRUA, CRUB, and CRUC homohexamers were 5.7, 6.0, and 5.0 °C, respectively, suggesting a more cooperative denaturation process than WT ($\Delta T_{1/2}$ = 6.9 °C) (Table 3). The strong interactions that may occur between the IE face of CRUC trimers, as discussed previously, may have contributed to the sharpest peak ($\Delta T_{1/2}$, 5.0 °C) observed for this homohexamer and indicative of a highly cooperative thermal denaturation process.

The difference between heat capacities of the native and unfolded states ($\Delta C_{pN\rightarrow U}$ value) for thermal denaturation of the homohexamers was positive and in the range 0.36−0.51 kJ K^{-1} mol^{-1} and did not differ significantly ($P > 0.05$) from WT heterohexamer (Table 3). Enthalpy (ΔH) at the transition temperature (T_m) of cruciferin unfolding was an endothermic process ($\Delta H_{Tm} > 0$) and could be calculated from the area beneath the denaturation peak. According to the enthalpy and entropy calculations (Table 3), ΔH_{Tm} values for cruciferins decreased in the order CRUC > WT > CRUA > CRUB with an opposite pattern observed for the entropy change (ΔS_{Tm}). Positive values for both enthalpy and entropy changes similar to that observed here generally represent high hydrophobic interactions in the molecule.[45] The highest ΔH_{expTm} value (181.6 kJ mol^{-1}) for the CRUC homohexamer further confirms the compact nature of this molecule, which may occur due to strong hydrophobic forces between two trimers leading to low conformational flexibility. The degree of disordered conformation for the CRUC homohexamer was high when the protein underwent thermal unfolding (ΔS_{Tm}, 0.47 kJ K^{-1} mol^{-1}) compared to the other cruciferin variants (Table 3). The unfolding and consequent exposure of the long HVR-I region of CRUC homohexamer to the solvent upon thermal denaturation could be attributed to its high disordering property. The two endothermic peaks (Supporting Information, Figure S4) seen with the CRU- protein could be for the large protein (cruciferin-like protein peak at 100.5 °C) and the trimeric form (at 91.8 °C) as observed in the native-PAGE (Figure 2A). The lowest enthalpy change (102.8 kJ mol^{-1}) for the large form of the CRU- protein (Table 3) may be explained to some degree by the low content of ordered secondary structure (Table 1).[22]

The van't Hoff enthalpy value (ΔH_{vHTm}, Table 3) can be used to describe the transition mode or cooperative unfolding

of cruciferins. When a protein undergoes a two-state transition from native state to an unfolded state (i.e., N↔U), the ratio of ΔH_{vHTm} to ΔH_{expTm} is unity and a deviation from unity can be caused by either the presence of intermediate molecules or oligomerization of the native or unfolded state.[46] Calculated values of $\Delta H_{vHTm}/\Delta H_{expTm}$ for WT heterohexamer and homohexameric cruciferins were equal to ∼1 (Table 3); therefore, it can be described as a two-state model, $N_{12}\leftrightarrow$ 12U, considering the number of monomers is 12 (α- and β-chains as separate units) for 11S cruciferin.[22] A two-state model for thermal unfolding of WT cruciferin has been reported and suggests that each monomer in cruciferin acts as a cooperative unit in the denaturation process.[4] In contrast, the protein of triple-knockout line deviated from this model, $\Delta H_{vHTm}/\Delta H_{expTm} < 1$ (Table 3), indicating existence of possible oligomers during the unfolding process.

Contribution of Each Subunit Type to WT Cruciferin. The present study and previous MS analysis of Wan et al.[29] support the notion that CRUC is the predominant cruciferin protomer species in *Arabidopsis*. The CRUC homohexamer isolated from the *CRUabC* mutant line had distinct structural and physicochemical properties compared to WT heterohexamer and to the cruciferins of the other double-knockout lines. Although we expected that the distinct properties of CRUC protomers may dominate in the WT heterohexamer, interestingly, this was not observed. Therefore, to elicit distinct surface charge, intrinsic hydrophobicity, surface hydrophobicity, structural stability, and thermal denaturation properties, CRUC has to be in its homohexameric composition. We show evidence that the CRUC protomers interact to form a very stable homohexamer assembly with a compact structure. The physicochemical properties of CRUA and CRUB homohexamers deviated from CRUC homohexamer in many ways, and structural differences must have contributed to this. The divergent properties of CRUC homohexamer observed here may be moderated when interacting with CRUA and CRUB protomers in WT cruciferin.

In summary, studying the details of the structure and physicochemical properties of homohexameric cruciferin obtained from mutant *Arabidopsis* lines allowed us to understand the contribution of CRUA, CRUB, and CRUC to these properties, and also to validate the predictions[10] of properties made for these molecules based *in silico* homology model analysis. The present study confirmed that the different structural characteristics of the CRUC protomer compared to CRUA and CRUB were reflected in the physicochemical properties of the respective hexamer and trimer. Our study also points out that the secondary structure components of these protomers are only slightly affected by this genetic variation, but that the tertiary and quaternary structure characteristics such as observed through zeta potential, thermal stability, structure stability, intrinsic fluorescence, and surface hydrophobicity which are directly related to the functions of cruciferin molecule are very much affected.

■ ASSOCIATED CONTENT

Supporting Information

Figures S1, S2, S3, and S4. This material is available free of charge via the Internet at http://pubs.acs.org.

■ AUTHOR INFORMATION

Corresponding Author

*Phone: (306) 956-7684. Fax: (306) 956-7247. E-mail: janitha.wanasundara@agr.gc.ca.

Notes

The authors declare no competing financial interest.

■ ACKNOWLEDGMENTS

This work was funded by the AAFC Canadian Crop Genomics Initiative. T.S.W.-G. was the recipient of the SaskCanola Dr. S. Roger Rimmer graduate scholarship. Dr. Michael Nickerson of University of Saskatchewan is acknowledged for instrument facilitation.

■ REFERENCES

(1) Tandang-Silvas, M. R. G.; Fukuda, T.; Fukuda, C.; Prak, K.; Cabanos, C.; Kimura, A.; Itoh, T.; Mikami, B.; Utsumi, S.; Maruyama, N. Conservation and divergence on plant seed 11S globulins based on crystal structures. *Biochim. Biophys. Acta* **2010**, *1804*, 1432−1442.

(2) Simon, A. E.; Tenbarge, K. M.; Scofield, S. R.; Finkelstein, R. R.; Crouch, M. L. Nucleotide sequence of a cDNA clone of *Brassica napus* 12S storage protein shows homology with legumin from *Pisum sativum*. *Plant Mol. Biol.* **1985**, *5*, 191−201.

(3) Rödin, J.; Ericson, M. L.; Josefsson, L. G.; Rask, L. Characterization of a cDNA clone encoding a *Brassica napus* 12S (cruciferin) subunit. Relationship between precursors and mature chains. *J. Biol. Chem.* **1990**, *265*, 2720−2723.

(4) Tandang, M. R. G.; Adachi, M.; Inui, N.; Maruyama, N.; Utsumi, S. Effects of protein engineering of canola procruciferin on its physicochemical and functional properties. *J. Agric. Food Chem.* **2004**, *52*, 6810−6817.

(5) Tandang, M. R. G.; Adachi, M.; Utsumi, S. Cloning and expression of rapeseed procruciferin in *Escherichia coli* and crystallization of the purified recombinant protein. *Biotechnol. Lett.* **2004**, *26*, 385−391.

(6) Tandang, M. R. G.; Atsuta, N.; Maruyama, N.; Adachi, M.; Utsumi, S. Evaluation of the solubility and emulsifying property of soybean proglycinin and rapeseed procruciferin in relation to structure modified by protein engineering. *J. Agric. Food Chem.* **2005**, *53*, 8736−8744.

(7) Dickinson, S. D.; Hussein, E. H. A.; Neilsen, N. C. Role of posttranslational cleavage in glycinin assembly. *Plant Cell* **1989**, *1*, 459−469.

(8) Adachi, M.; Takenaka, Y.; Gidamis, A. B.; Mikami, B.; Utsumi, S. Crystal structure of soybean proglycinin A1aB1b homotrimer. *J. Mol. Biol.* **2001**, *305*, 291−305.

(9) Maruyama, N.; Prak, K.; Motoyama, S.; Choi, S.-K.; Yagasaki, K.; Ishimoto, M.; et al. Structure-physicochemical function relationships of soybean glycinin at subunit levels assessed by using mutant lines. *J. Agric. Food Chem.* **2004**, *52*, 8197−8201.

(10) Withana-Gamage, T. S.; Hegedus, D. D.; Qiu, X.; Wanasundara, J. P. D. In silico homology modeling to predict functional properties of cruciferin. *J. Agric. Food Chem.* **2011**, *59*, 12925−12938.

(11) Withana-Gamage, T. S.; Hegedus, D. D.; Qiu, X.; Yu, P.; May, T.; Lydiate, D.; Wanasundara, J. P. D. Characterization of *Arabidopsis thaliana* lines with altered seed storage protein profiles using synchrotron powered FT-IR. *J. Agric. Food Chem.* **2013**, *61*, 901−912.

(12) Bérot, S.; Compoint, J. P.; Larré, C.; Malabat, C.; Guéguen, J. Large scale purification of rapeseed proteins (*Brassica napus* L). *J. Chromatogr., B: Anal. Technol. Biomed. Life Sci.* **2005**, *818*, 35−42.

(13) Wanasundara, J. P. D.; Abeysekara, S. J.; McIntosh, T. C.; Falk, K. C. Solubility differences of major storage proteins of Brassicaceae oilseeds. *J. Am. Oil Chem. Soc.* **2012**, *89*, 869−881.

(14) AOCS Official Method Am 2−93, Determination of Oil Content in Oilseeds. *In Official Methods and Recommended Practices of the AOCS*, 5th ed.; Firestone, D. E., Ed.; AOCS Press: Champaign, IL, 1997.

(15) Lonien, J.; Schwender, J. Analysis of metabolic flux phenotypes for two Arabidopsis mutants with severe impairment in seed storage lipid synthesis. *Plant Physiol.* **2009**, *151*, 1617−1634.
(16) Kauppinen, J. K.; Moffatt, D. J.; Mantsch, H. H.; Cameron, D. G. Fourier self-deconvolution: A method for resolving intrinsically overlapped bands. *Appl. Spectrosc.* **1981**, *35*, 271−276.
(17) Byler, D. M.; Susi, H. Examination of the secondary structure of proteins by deconvolved FTIR spectra. *Biopolymers* **1986**, *25*, 469−487.
(18) Dong, A.; Huang, P.; Caughey, W. S. Protein secondary structures in water from second-derivative amide I infrared spectra. *Biochemistry* **1990**, *29*, 3303−3308.
(19) Whitmore, L.; Wallace, B. A. Protein secondary structure analysis from circular dichroism spectroscopy: Methods and reference databases. *Biopolymers* **2008**, *89*, 392−400.
(20) Stern, V. O.; Volmer, M. On the quenching-time of fluorescence. *Phys. Z.* **1919**, *20*, 183−188.
(21) Kato, A.; Nakai, S. Hydrophobicity determined by a fluorescence probe method and its correlation with surface properties of proteins. *Biochim. Biophys. Acta* **1980**, *624*, 13−20.
(22) Koshiyama, I.; Hamano, M.; Fukushima, D. A heat denaturation study of the 11S globulin in soybean seeds. *Food Chem.* **1981**, *6*, 309−322.
(23) Privalov, P. L.; Potekhin, S. A. Scanning microcalorimetry in studying temperature-induced changes in proteins. *Methods Enzymol.* **1986**, *131*, 4−51.
(24) *SAS User's Guide: Statistical Analysis System*; SAS Institute Inc.: Cary, NC, 2004.
(25) Hansen, M.; Lange, M.; Friis, C.; Dionision, G.; Holm, P. B.; Vincze, E. Antisense-mediated suppression of C-hordein biosynthesis in the barley grain results in correlated changes in the transcriptome, protein profile, and amino acid composition. *J. Exp. Bot.* **2007**, *58*, 3987−3995.
(26) Pandurangan, S.; Pajak, A.; Moinar, S. J.; Cober, E. R.; Dhaubhadel, S.; Hernández-Sebastia, C.; et al. Relationship between asparagine metabolism and protein concentration in soybean seed. *J. Exp. Bot.* **2012**, *63*, 3173−3184.
(27) Inquello, V.; Raymond, J.; Azanza, J. L. Disulfide interchange reactions in 11S globulin subunits of Cruciferae seeds. Relationships to gene families. *Eur. J. Biochem.* **1993**, *217*, 891−895.
(28) Rödin, J.; Rask, L. Characterization of the 12S storage protein of *Brassica napus* (cruciferin): Disilfide bonding between subunits. *Physiol. Plant.* **1990**, *79*, 421−426.
(29) Wan, L.; Ross, A. R. S.; Yang, J.; Hegedus, D. D.; Kermode, A. R. Phosphorylation of the 12S globulin cruciferin in wild-type and abi1-1 mutant *Arabidopsis thaliana* (thale cress) seeds. *Biochem. J.* **2007**, *404*, 247−256.
(30) Yamagishi, T.; Miyakawa, A.; Noda, N.; Yamauchi, F. Isolation and electrophoretic analysis of heat induced products of mixed soybean 7S and 11S globulins. *Agr. Biol. Chem.* **1983**, *47*, 1229−1237.
(31) Miyazawa, T.; Shimanouchi, T.; Mizushima, S. Characteristic infrared bands of monosubstituted amides. *J. Chem. Phys.* **1956**, *24*, 408−418.
(32) Susi, H. Infrared spectroscopy-conformation. *Methods Enzymol.* **1972**, *26*, 455−472.
(33) Manavalan, P.; Johnson, W. C., Jr. Sensitivity of circular dichroism to predict tertiary structure class. *Nature* **1983**, *305*, 831−832.
(34) Gerbanowski, A.; Malabat, C.; Rabiller, C.; Guéguen, J. Grafting of aliphatic and aromatic probes on rapeseed 2S and 12S proteins: Influence on their structural and physicochemical properties. *J. Agric. Food Chem.* **1999**, *47*, 5218−5226.
(35) Sze, K. W. C.; Kshirsagar, H. H.; Venkatachalam, M.; Sathe, S. K. A circular dichroism and fluorescence spectrometric assessment of effects of selected chemical denaturants on soybean (*Glycine max* L.) storage proteins glycinin (11S) and β-conglycinin (7S). *J. Agric. Food Chem.* **2007**, *55*, 8745−8753.
(36) Henriksson, G.; Englund, A. K.; Johansson, G.; Lundahl, P. Calculation of the isoelectric points of native proteins with spreading of p*Ka* values. *Electrophoresis* **1995**, *16*, 1377−1380.
(37) Chen, Y.; Barkley, M. D. Towards understanding tryptophan fluorescence in proteins. *Biochemistry* **1998**, *37*, 9976−9982.
(38) Dufour, E.; Hoa, G. H.; Haertlé, T. High-pressure effects of β-lactoglobulin interactions with ligands studied by fluorescence. *Biochim. Biophys. Acta* **1994**, *1206*, 166−172.
(39) Lakowicz, J. R. *Principles of Fluorescence Spectroscopy*, 3rd ed.; Springer: New York, 1999.
(40) Lehrer, S. S. Solute perturbation of protein fluorescence the quenching of tryptophan fluorescence of model compounds and of lysozyme by iodide ion. *Biochemistry* **1971**, *17*, 3254−3263.
(41) Marcone, M. F.; Yada, R. Y.; Kakuda, Y. Evidence for a molten globule state in an oligomeric plant protein. *Food Chem.* **1997**, *60*, 623−631.
(42) Haskard, C. A.; Li-Chan, E. C. Y. Hydrophobicity of bovine serum albumin and ovalbumin determined using uncharged (PRODAN) and anionic (ANS^-) fluorescent probes. *J. Agric. Food Chem.* **1998**, *46*, 2671−2677.
(43) Damodaran, S. Amino acids, peptides and proteins. In *Fennema's Food Chemistry*; Damodaran, S., Parkin, K. L., Fennema, O. R., Eds.; CRC Press: Boca Raton, FL, 2008; Vol. *4*, pp 217−329.
(44) Privalov, P. L.; Khechinashvili, N. N. A thermodynamic approach to the problem of stabilization of globular protein structure: A calorimetric study. *J. Mol. Biol.* **1974**, *86*, 665−v684.
(45) Tian, J.; Liu, J.; He, W.; Hu, Z.; Yao, X.; Chen, X. Probing the binding of scutellarin to human serum albumin by circular dichroism, fluorescence spectroscopy, FTIR, and molecular modeling method. *Biomacromolecules* **2004**, *5*, 1956−1961.
(46) Makhatadze, G. I. Measuring protein thermostability by differential scanning calorimetry. In *Current Protocols in Protein Chemistry*; Coligan, J. E., Dunn, B. M., Ploegh, H. L., Speicher, D. W., Wingfield, P. T., Eds.; Wiley: New York, 1998; Vol. *2*, pp 7.9.1−7.9.14.